

SciEn Conference Series: Engineering Vol. 3, 2025, pp 137-142

https://doi.org/10.38032/scse.2025.3.33

# Biogenic Synthesis of Ni-doped Iron Oxide ( $Fe_2O_3$ ) Nanoparticles from *Hibiscus Sabdariffa* (Rosella) Leaf Extract and Investigating their Antibacterial Activity

Md. Lael Hasan, Hridoy Roy, Md. Estabrak Ahammod Sakib\*, Md. Farhan Muskan

Department of Glass & Ceramic Engineering, Rajshahi University of Engineering & Technology, Rajshahi-6204, Bangladesh

# **ABSTRACT**

Iron oxide  $(Fe_2O_3)$  nanoparticles have various types of applications and in this era, biogenic synthesis is the most effective and eco-friendly method to synthesize the nanoparticles. This research aimed to synthesize the Ni-doped Iron oxide nanoparticles by using leaf extract of *Hibiscus Sabdariffa* (Rosella), Iron (III) nitrate nonahydrate as the source of Iron, and Nickle nitrate hexahydrate as the source of Nickle. The synthesized nanoparticles were analyzed through various techniques such as X-ray diffraction (XRD), scanning electron microscopy (SEM), and UV-visible spectroscopy to determine their structural, morphological, and optical properties. XRD result of NPs confirmed the formation of crystalline iron oxide NPs and Ni-doped iron oxide NPs with the average crystalline size of 13.90 nm and 14.94 nm respectively. SEM analysis provided NPs insights into the surface morphology and particle size, revealing spherical nanoparticles size between 10 nm to 90 nm, with average spherical size of iron oxide NPs and Ni-doped NPs is 46.13 nm  $\pm$  4.71 nm and 35.27 nm  $\pm$  1.32 nm respectively. UV visible spectroscopy analysis showed the absorbance and energy band gap of both nanoparticles. Antibacterial activity revealed variations in the zone of inhibition between pure iron oxide NPs and Ni-doped iron oxide NPs. This biogenic method is not only eco-friendly but also cost-effective with its various types of potential applications.

Keyword: Biogenic Synthesis, Iron oxide nanoparticles, Rosella leaf, Hibiscus Sabdariffa, Antibacterial activity.



Copyright @ All authors

This work is licensed under a Creative Commons Attribution 4.0 International License.

# 1. Introduction

Nanotechnology is one of the advanced techniques employed in many chemical and physical processes for the fabrication of nanomaterials with identical properties [1], [2]. This technique helps the formation of new materials in the nano range under 100 nm. The nonmaterial has some potential applications such as nanomedicine, biomaterials, sensors, drug delivery systems, nanoelectronics, agriculture, information and communication, and heavy industry [3], [4].

Among the various types of nanoparticles, Iron oxide nanoparticles achieved earmarked attention to the researcher due to their identical properties like superparamagnetism, low susceptibility to oxidation, firmness with a wide range of applications like drug delivery system, antibiotic degradation, magnetic cell sorting, magnetic particle imaging (MPI), adsorption of dyes, biosensing, and bioengineering [5-15]. The magnetic properties of iron oxide nanoparticles could be improved by doping with transition metals like Ni, Co, and Mn [16]. In this research, Ni is used as a doping metal to synthesize the iron oxide nanoparticles which exhibit superparamagnetic properties at room temperature [16], [17]. When Ni doped into the iron oxide nanoparticles it would form a spinel structure of nickel ferrite. It also contains a cubic structure where tetrahedral and octahedral sites are occupied at different positions [16]. Effective doping of transition metal has been achieved through various techniques like electrodeposition [18], chemical deposition [19], spin coating [20], spray pyrolysis

[21], and green synthesis process [22]. 5 wt% Ni was used in iron oxide by green synthesis, which is a cost-effective, eco-friendly, and simple process [23]. *Hibiscus Sabdariffa* (Rosella) leaf extract is used as a green object that contains flavonoid [24], anthocyanin, glucoside hibiscus, lignin, organic acid, and glossy pepsin [24] and exhibits identical properties as antiseptic, antioxidant, antibacterial, and diuretic properties [25], [26].

Further, the synthesized iron oxide and Ni-doped iron oxide nanoparticles is characterized by XRD analysis, SEM analysis, UV-visible spectroscopy analysis, and antibacterial activity variation. Significance of this research to investigate the Ni doped iron oxide NPs antibacterial activity, the research address the growing demand for novel antimicrobial agent. This nanoparticle hold their potential application for diverse application, including medical treatment, water purification, and environmental remediation.

# 2. Materials and Methods

#### 2.1. Materials

For the synthesis process the materials required are: Iron (III) Nitarte Nonahydrate ( $Fe(NO_3)_3$ .9 $H_2O$ , Purity: 98%, Origin: India), Nickle Nitrate Hexahydrate ( $Ni(NO_3)$ .6 $H_2O$ , Purity: 98%, Origin: India). All the materials used were of analytical grade.

# 2.2. Preparation of *Hibiscus Sabdariffa* (Rosella) leaf Extract

Rosella leaf was collected from the local area of Rajshahi and washing it through de-ionized water. 30g of choppedleaf was added into 300 ml of de-ionized water and heated it 30 min at 80°C. The resulting solution was filtered through WHATMAN NO-1 filter paper to remove the residue. The filtered extract was kept at 4°C for further use.

# 2.3. Synthesis of Ni-doped Iron Oxide NPs

Iron (III) nitrate nonahydrate is used as the source of Iron, and Nickel nitrate hexahydrate is used as the source of Nickel. At room temperature, 150ml of Hibiscus Sabdariffa (Rosella) leaf Extract was added into the 2M 100ml of Iron (III) nitrate nonahydrate to prepare the solution. After 30 min of adding Iron (III) nitrate nonahydrate, 5 wt% Nickle nitrate hexahydrate was added to the solution. The solution was stirred with a magnetic stirrer for 3 hours at 80°C. The color change (Red Brown) of the solution indicated the formation of nanoparticles. The resulting solution was centrifuged for 15 min at 5000 rpm and washed the solution twice times through a 5% ethanol solution. The sample of NPs was dried at 100°C overnight in a laboratory oven. After drying, the powder was calcined at 550°C for 6 hours. Finally, the obtained Ni-doped iron oxide nanoparticles were kept in a glass bottle for further characterization. Fig. 1 shows the process of Ni-doped iron oxide fabrication.



**Fig.1** Process flow diagram of Ni-doped  $Fe_2O_3$  NPs.

# 2.4 Characterization

Structural characterization of both NPs was done by using X-ray diffraction, which is conduct by Bruker's D8 (Germany) advanced diffractometer by engaging 40kV-40ma Cu-K $\alpha$  radiation and scanning electron microscopy (SEM) used for morphological analysis with scanning speed 2.0000 (deg/min). Elemental characterization was done by energy dispersive X-ray (EDS) technique. Both of these conducted by ZEISS EVO 18 (UK). All UV-visible

spectra were recorded on the T80+ double-beam UV-visible spectrophotometer (Range: 190-1100nm). The absorption spectra of both nanoparticles were recorded by dispersion in aqueous solution and scanned in the range 200-800 nm.

The Antibacterial Activity of synthesized NPs was evaluated through *Staphylococcus aureus* as gram-positive bacteria and *E. Coli* as gram-negative bacteria by using the disk

diffusion method [27]. All the bacteria were placed in an agar plate around 6 mm in diameter and 4mg NPs were placed into the wells. Finally, the plate was incubated at 37°C for 24hr. After the incubation, the zone of inhibition was measured.

#### 3. Result and Discussion

# 3.1. XRD Analysis

XRD analysis was used to find out the crystalline and structural characteristics of Hibiscus Sabdariffa (Rosella) leaf synthesizes iron oxide( $Fe_2O_3$ ) NPs and Ni-doped iron oxide NPs. Fig.2 shows the XRD pattern for both of the NP which is obtained after the calculations at 550°C and indicates the purity and proper phase formation of both of the NPs. In this study, only 5 wt% Ni was doped into the pure iron oxide NPs. There is no change in the lattice parameter due to almost the same size of the dopant Ni ion (0.7 Å) and the host ion Fe (0.77 Å)[28]. Due to the doping of Ni ions into the pure NPs, a broadening diffraction peak was observed. The doping attribute is the size reduction of particle [23]. Due to the lower size of dopant, it will take place in host lattice's interstitial position. The observed intensity peak which represents the corresponding plane for both NPs from the JCPDS card no 96-900-5827.

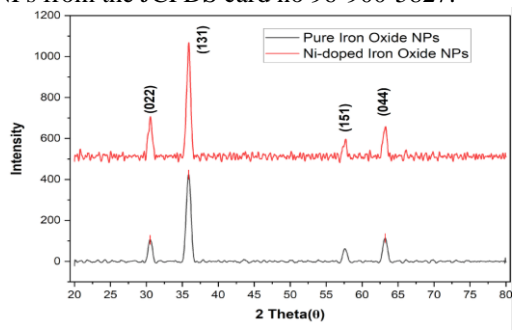


Fig.2 XRD pattern of both NPs.

The average crystalline size of the sample was find out by the Debye The average crystalline size of the sample was find out by the Debye-scherrer equation,

$$d = (\frac{k\lambda}{\beta \cos \theta}) \tag{1}$$

Where d is the crystalline size, k is the scherrer constant (0.98),  $\lambda$  is the wavelength (1.54 nm),  $\beta$  denotes the full width at half maximum (FWHM) and  $\theta$  = Bragg angle. The average crystalline size is shown in the Table 1.

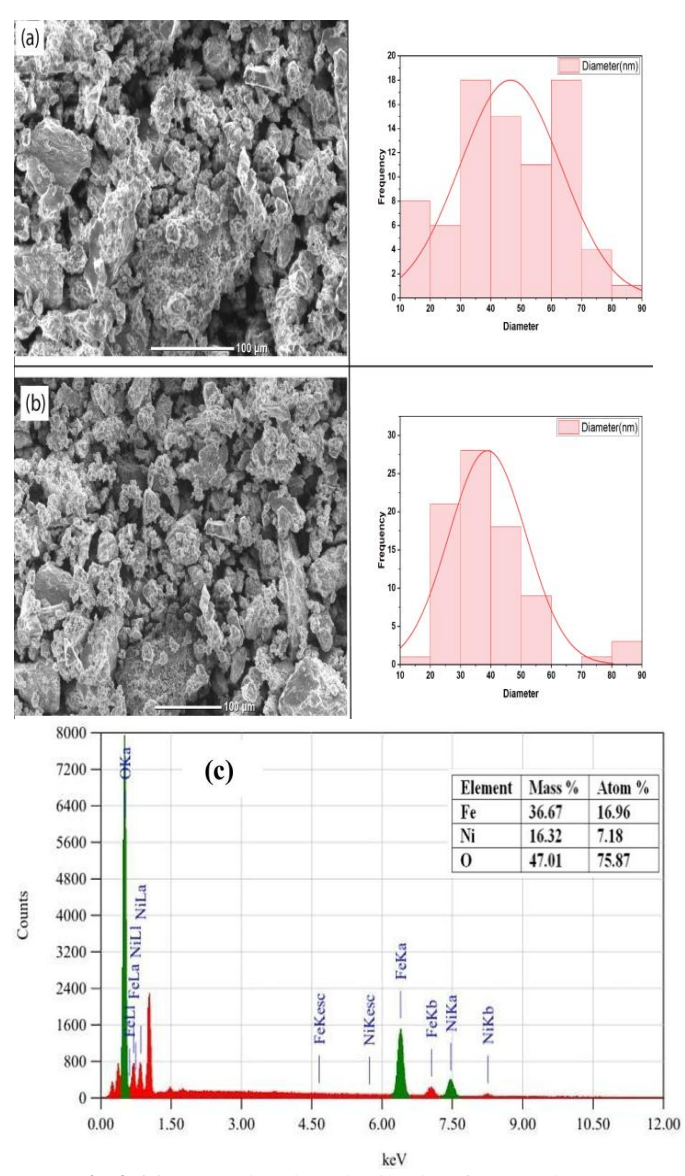
**Table 1** Crystalline size of both NPs

Table 1 Crystalline size of both NFs						
NPs	$(2\theta)$	<b>FWHM</b>	Crystalline	Average		
			Size D (nm)	(nm)		
Pure	30.52	0.61	14.09			
NPs	35.58	0.73	11.93	13.90		
	57.34	0.62	15.24			
	63.48	0.68	14.34			
Ni-	30.54	0.64	13.43			
doped	35.96	0.61	14.29	14.94		
NPs	57.72	0.58	16.32			
	63.18	0.62	15.70			

# 3.2. SEM with EDS Analysis

Fig. 3 shows the FE-SEM image of iron oxide  $(Fe_2O_3)$  and Ni-doped iron oxide nanoparticles and the shape and surface

morphology properties of the biogenic synthesis of nanoparticles. The image of SEM shows that the nanoparticles exhibit a non-uniform irregular shape and a few hexagonal particles shaped with a narrow size distribution of 10-90 nm [29]. The average size of the particles for iron  $oxide(Fe_2O_3)$  NPs and Ni-doped iron oxide( $Fe_2O_3$ ) NPs is 46.13 nm  $\pm$  4.71 nm and 35.27 nm  $\pm$ 1.32 nm, respectively. Due to the addition of 5 wt% Ni in pure iron oxide NPs, the particle size decreases. Ni doping in pure oxide NPs can undoubtedly stop the development of particles and reduce the size of particles [22]. Fig. 3(c) shows the EDS peak spectrum of NPs with the amount of Fe, Ni, and O elements. The sharp peaks observed between 0.00 keV to 1.50 keV, and 6.00 keV to 7.50keV are correlated to crystalline NPs and small size particle enhance the high surface area which helps to increase the inhibition against bacteria.



**Fig.3** (a)SEM with size distribution for pure iron oxide( $Fe_2O_3$ ) NPs (b) SEM with size distribution for Nidoped iron oxide( $Fe_2O_3$ ) NPs(c) EDS analysis

# 3.3. UV-visible spectroscopy analysis

UV-visible spectroscopy is a powerful technique to explore the optical properties of semiconducting nanoparticles. The absorption spectra of pure iron  $\text{oxide}(Fe_2O_3)$  NPs and Nidoped $Fe_2O_3$  NPs are shown in Fig.4 which is depend on the

surface roughness, impurity centers, and band gap [23]. The observed absorption value for pure Iron oxide NPs and Nidoped iron oxide NPs are 256.5 nm and 268.6 nm respectively. The tauc plot is constructed by plotting  $(\alpha h \theta)$ vs.  $h\theta$  (where  $\alpha$  is the coefficient of absorbance and  $h\theta$  is the energy of photon), and this graph is driven by the UVvisible absorption data. The measure band gap found to be 4.06 eV for pureIron oxide  $(Fe_2O_3)$  NPs and 3.24 eV for Nidoped iron  $oxide(Fe_2O_3)$  NPs. Due to the doping of Ni, it reduce the band gap energy even the particle size reduction. This decrease in band gap energy is not related to the size of a particle may be due to Ni dopant migrates toward to the base lattice  $Fe_2O_3$  and form a localized energy between the valence band and conduction band and reducing the band gap. It indicates that the NPs have potential ability to photocatalytic degradation of dye under solar light irradiation [30].

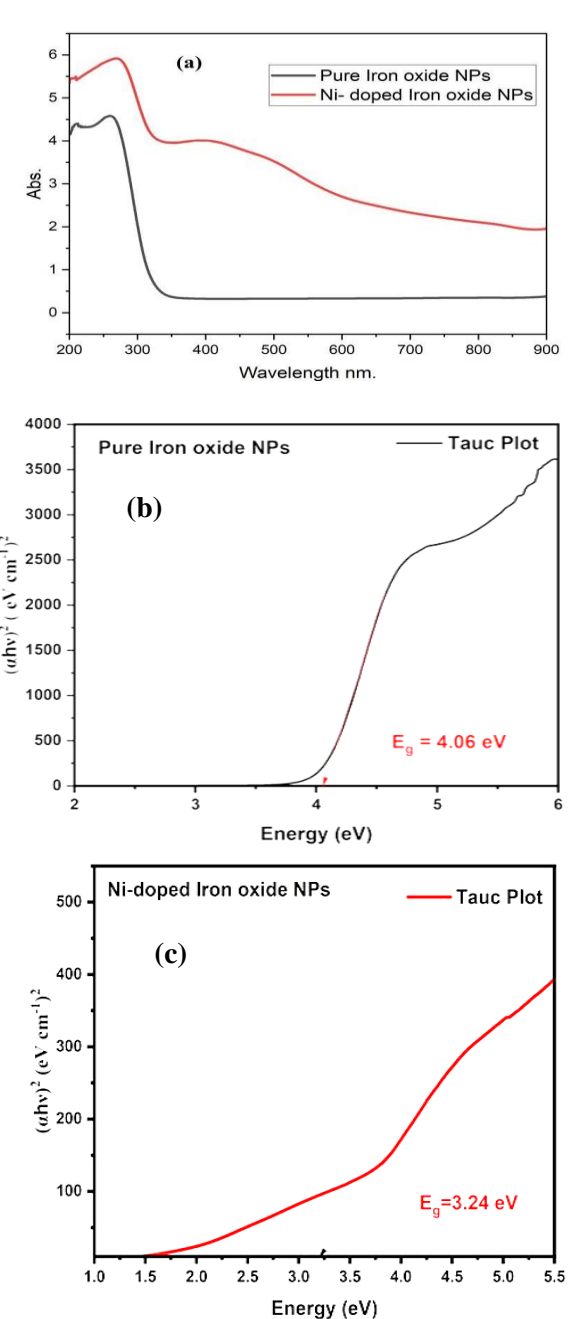


**Fig.4(a)**Absorbance value of both NPS **(b)**Tauc plot for band gap energy of Pure $Fe_2O_3$  NPs **(c)**Tauc plot for band gap energy of Ni-doped $Fe_2O_3$  NPs.

# 3.4. Antibacterial Activity Analysis

The agar wall diffusion method was used to investigate the antibacterial activity of both nanoparticles. *Staphylococcus aureus* is used as gram positive bacteria and *E. Coli* is used as a gram negative bacteria for both NPs. Table 2 shows the result of the zone of inhibition for both bacteria. The zone of inhibition values were recorded and it shows that the bacterial cell are highly inhibited by both of this NPs. *Staphylococcus aureus* is much more inhibited than *E. Coli* which is observed for variation of cell wall structure [31]. Due to the addition of Ni in pure NPs the zone of inhibition will increase the production of ROS due to oxidative stress in microbial cells and damaging bacterial cell membranes and DNA (Fig. 6). Also, the zone of inhibition increases due to the change in the morphology of nanoparticles. Fig.5 shows the analysis graph for both NPs.

Table 2 Zone of Inhibition of both NPs

Disk	Zone of Inhibition (ZOI)						
$(\mu g/$	Pure Iron Oxide NPs		Ni-doped Iron Oxide				
disc)	NPs						
	S. aureus	E. Coli	S. aureus	E. Coli			
50	7	7	7	7.5			
100	7	7.5	8	8			
150	14	12	16.5	12.5			
200	21	17	23	18.5			

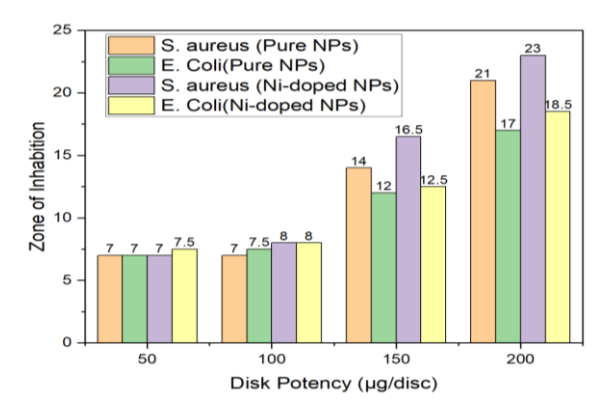


Fig.5 Antibacterial Activity of synthesize both NPs.

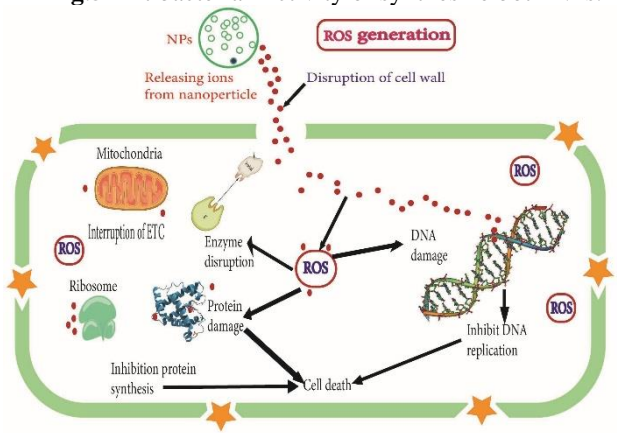


Fig.6 Antibacterial Activity Mechanism

# 4. Conclusion

Ni-doped iron oxide nanoparticles have been successfully done by the biogenic synthesis method by using *Hibiscus Sabdariffa* (Rosella) Leaf Extract. The XRD analysis confirms the formation of NPs and shows the average crystalline size. SEM analysis provides the surface

morphology with particle size distribution indicates the reducing of particle dimension due to doping. Due to the reduction of particles by doping Ni, the energy band gap reduced from 4.06 eV to 3.24 eVas observed by UV-visible analysis. Also, the Ni-doped iron oxide shows a better result against both gram-positive and gram-negative bacteria which shows effectiveness as a coating on medical devices, drug delivery systems, and water purification, and reduces antibiotic resistance. The study reinforces the significance of green synthesis as a sustainable method for developing functional nanomaterials with diverse industrial and medical application.

#### References

- [1] Singh Y, Kaur A, Suri B and Singhal S. "Systematic literature review on regression test prioritization techniques", Informatica, Vol. 36, pp. 379–408, 2012.
- [2] Hafeez, M., Shaheen, R., Akram, B., Zain-Ul-Abdin, N., Haq, S., Mahsud, S., Ali, S., & Khan, R. T." Green synthesis of cobalt oxide nanoparticles for potential biological applications." Materials Research Express, Vol.7, No. 2, 2020.
- [3] Buzea, C., Pacheco, I. I., & Robbie, K., "Nanomaterials and nanoparticles: Sources and toxicity", Biointerphases, Vol. 2, No.4, MR17–MR71, 2017.
- [4] Athawale A A, Majumdar M, Singh H and Navinkiran K 2010 Synthesis of cobalt oxide nanoparticles/fibres in alcoholic medium using yray technique Def. S. J. 60 507–13.
- [5] Priya, N., Naveen, N., Kaur, K., & Sidhu, A. K. "Green Synthesis: An Eco-friendly Route for the Synthesis of Iron Oxide Nanoparticles." Frontiers in Nanotechnology, Vol. 3, 2021
- [6] Ali Talha Khalil, Muhammad Ovais, Ikram Ullah, Muhammad Ali, Zabta Khan Shinwari, Malik Maaza, "Biosynthesis of iron oxide (Fe2O3) nanoparticles via aqueous extracts of Sageretia thea (Osbeck.) and their pharmacognostic properties", Green Chemistry Letters and Reviews, Vol. 10, No. 4, pp. 186–201, 2017.
- [7] Nasrin Beheshtkhoo, Mohammad Amin Jadidi Kouhbanani, Amir Savardashtaki, Ali Mohammad Amani, Saeed Taghizadeh, "Green synthesis of iron oxide nanoparticles by aqueous leaf extract of Daphne mezereum as a novel dye removing material", Applied Physics A, Vol. 124, No. 5, 2018.
- [8] P. Durga Sruthi, Chamarthy Sai Sahithya, C. Justin, C. SaiPriya, Karanam Sai Bhavya, P. Senthilkumar and Antony V. Samrot, "Utilization of Chemically Synthesized Super Paramagnetic Iron Oxide Nanoparticles in Drug Delivery, Imaging and Heavy Metal Removal", Journal of Cluster Science, Vol. 30, No. 1, pp. 11–24, 2019.
- [9] Zhang, R., Zhou, Y., Yan, X., & Fan, K, "Advances in chiral nanozymes: a review", *Microchimica Acta*, Vol. 186, No. 782, pp. 1-12, 2019.
- [10] Md. Shakhawat Hossen Bhuiyan, Muhammed, Yusuf Miah, Shujit Chandra Paul, Tutun

- Das Aka, Otun Saha, Md. Mizanur Rahaman, Md. Jahidul Islam Sharif, Ommay Habiba and Md. Ashaduzzaman, "Green synthesis of iron oxide nanoparticle using Carica papaya leaf extract: application for photocatalytic degradation of remazol yellow RR dye and antibacterial activity", Heliyon, Vol. 6, No. 8, p. e04603, 2020.
- [11] Gao, L., Fan, K., Yan, X., Iron Oxide Nanozyme: A Multifunctional Enzyme Mimetics for Biomedical Application. In: Yan, X. (eds) Nanozymology. Nanostructure Science and Technology. Springer, Singapore, pp. 105-140, 2020.
- [12] Malhotra, N., Lee, J.-S., Liman, R. A. D., Ruallo, J. M. S., Villaflores, O. B., Ger, T.-R., & Hsiao, C.-D., "Potential Toxicity of Iron Oxide Magnetic Nanoparticles: A Review", Molecules, Vol. 25, Issue 14, p. 3159, 2020.
- Piyal Mondal, A. Anweshan, and Mihir Kumar Purkait, "Green synthesis and environmental application of iron-based nanomaterials and nanocomposite: A review", Chemosphere, Vol. 259, p. 127509, 2020
- [14] Vasantharaj, S., Sathiyavimal, S., Senthilkumar, P., LewisOscar, F., & Pugazhendhi, A., "Biosynthesis of iron oxide nanoparticles using leaf extract of Ruellia tuberosa: Antimicrobial properties and their applications in photocatalytic degradation", Journal of Photochemistry and Photobiology B: Biology, Vol. 192, pp. 74–82, 2019.
- [15] Tong, W., Hui, H., Shang, W., Zhang, Y., Tian, F., Ma, Q., Yang, X., Tian, J., & Chen, Y., "Highly sensitive magnetic particle imaging of vulnerable atherosclerotic plaque with active myeloperoxidase-targeted nanoparticles", Theranostics, Vol. 11, No. 2, pp. 506–521, 2021. Moharana, A., Kumar, D., & Kumar, A.,
- [16] "Synthesis of Ni doped iron oxide nanoparticles and their dielectric properties", Journal of Physics: Conference Series, Vol. 1531, No. 1, p. 012113, 2020.
- [17] Francis Leonard Deepak, Manuel Bañobre-López, Enrique Carbó-Argibay, M. Fátima Cerqueira, Yolanda Piñeiro-Redondo, José Rivas, Corey M. Thompson, Saeed Kamali, Carlos Rodríguez-Abreu, Kirill Kovnir, and Yury V. Kolen'ko, "A Systematic Study of the Structural and Magnetic Properties of Mn-, Co-, and Ni-Doped Colloidal Magnetite Nanoparticles", The Journal of Physical Chemistry C, Vol. 119, No. 21, pp.11947-11957, 2015.
- [18] Yong-Sheng Hu, Alan Kleiman-Shwarsctein, Arnold J. Forman, Daniel Hazen, Jung-Nam Park, and Eric W. McFarland, "Pt-doped α-Fe2O3 thin films active for photoelectrochemical water splitting", *Chemistry of Materials*, *Vol.* 20, No. 12, pp.3803–3805, 2008.
- [19] S. Park, H.J. Kim, C.W. Lee, H.J. Song, S.S. Shin, S.W. Seo, H.K. Park, S. Lee, D.- W. Kim, K.S. Hong, "Sn self-doped -Fe2O3 nanobranch arrays supported on a transparent, conductive SnO2 trunk to improve photoelectrochemical

- water oxidation", International Journal of Hydrogen Energy, Vol. 39, No. 29, pp.16459–16467, 2014.
- [20] J. Frydrych, L. Machala, J. Tucek, K. Siskova, J. Filip, J. Pechousek, K. Safarova, M. Vondracek, J.H. Seo, O. Schneeweiss, M. Gr. Atzel, K. Sivula, R. Zboril, "Facile fabrication of tin-doped hematite photoelectrodes effect of doping on magnetic properties and performance for light-induced water splitting", Journal of Materials Chemistry, Vol.22, No. 43, pp. 23232-23239, 2012
- [21] J. Engel, H.L. Tuller, "The electrical conductivity of thin film donor doped hematite: from insulator to semiconductor by defect modulation", Physical Chemistry Chemical Physics, Vol. 16, No. 23, pp. 11374–11380, 2014.
- [22] Thakur, N., Kumar, P., Tapwal, A., & Jeet, K., "Degradation of malachite green dye by capping polyvinylpyrrolidone and Azadirachta indica in hematite phase of Ni doped Fe2O3 nanoparticles via co-precipitation method", Nanofabrication, Vol. 8, 2023.
- [23] Gattu, K. P., Ghule, K., Kashale, A. A., Patil, V. B., Phase, D. M., Mane, R. S., Han, S. H., Sharma, R., & Ghule, A. V., "Bio-green synthesis of Ni-doped tin oxide nanoparticles and its influence on gas sensing properties", RSC Advances, Vol. 5, No. 89, pp. 72849–72856, 2015.
- [24] Indryani Fauhan, K., Ehrich Lister, I. N., & Fachrial, E., "The Use of Rosella (Hibiscus sabdariffa L.) Extract Cream to Prevent Decreasing of Total Collagen in the Skin of Wistar Rats Exposed to Ultraviolet-B Light", Journal of Pharmaceutical Research International, Vol. 35, No. 1, pp. 24–32, 2023.
- [25] Vitri Nurilawaty, Tedi Purnama, Ai Emalia Sukmawati2, Silvester Maximus Tulandi, "The Potential of Rosella Floss (Hibiscus Sabdariffa l.) as a Dental Plaque Disclosing Agent", Journal of International Dental and Medical Research, Vol. 16, No. 4, pp. 1454-1461, 2023.
- [26] Fitriaturosidah, I., Kusnadi, J., Nurnasari, E., Nurindah, & Hariyono, B., "Phytochemical screening and chemical compound of green roselle(Hibiscus sabdariffa L.) and potential antibacterial activities", IOP Conference Series: Earth and Environmental Science, Vol. 974, No. 1, p. 012118, 2022.
- [27] Bauer, A.W., Kirby, W.M.M., Sherris, J.C., Truch, M., "Antibiotic susceptibility testing by standardized single disk method", American Journal of Clinical Pathology, Vol. 45, No. 4, pp. 493–496, 1996.
- [28] Asma Almontasser, Azra Parveen, "Probing the effect of Ni, Co and Fe doping concentrations on the antibacterial behaviors of MgO nanoparticles", Scientific Reports, Vol. 12, No. 1, pp. 1-33, 2022.
- [29] Deepthi, S., Vidya, Y. S., Manjunatha, H. C., Sridhar, K. N., Manjunatha, S., Munirathnam, R., Shivanna, M., kumar, S., & Ganesh, T., "Green photoluminescence, supercapacitor and cytotoxic properties of nickel doped haematite

- nanoparticles", Chemical Physics Impact, Vol. 9, p. 100708, 2024.
- [30] T. Kamakshi, G. Sunita Sundari, Harikrishna Erothu, Subhakaran Singh Rajaputra, "Effect of nickel dopant on structural, morphological and optical characteristics of Fe3O4 nanoparticles" Rasayan Journal of Chemistry, Vol. 12, No. 2, pp. 531-536, 2019.
- [31] Velsankar, K., Parvathy, G., Mohandoss, S., Krishna Kumar, M., & Sudhahar, S., "Celosia argentea leaf extract-mediated green synthesized iron oxide nanoparticles for bio-applications",

Journal of Nanostructure in Chemistry, Vol. 12, No. 4, pp. 625–640, 2021.

# **NOMENCLATURE**

 $\lambda$ : Wavelength of the X-rays, nm  $\theta$ : Bragg's Diffraction angle

D: Crystallite size, nm

 $\beta$ : Full width half maximum of intensity, radian

h: Planck's constant, J·s

Eg : Optical band gap energy, eV

α : Absorption coefficient